Ecological Complexity 7 (2010) 234–242

Contents lists available at ScienceDirect

Ecological Complexity

journal homepage: www.elsevier.com/locate/ecocom

Characterization of spatial scaling relationships between vegetation pattern and topography at different directions in Gurbantunggut desert, China

Jiangbo Xie [a,b,c], Tong Liu [a,*]

[a] College of Life Science, Shihezi University, Shihezi 832000, China
[b] Fukang Station of Desert Ecology, Xinjiang Institute of Ecology and Geography, Chinese Academy of Sciences, 40-3 South Beijing Road, Urumqi, Xinjiang 830011, China
[c] Graduate School, Chinese Academy of Sciences, 19A, Yu-Quan Road, Beijing 100049, China

ARTICLE INFO

Article history:
Received 14 December 2009
Received in revised form 8 February 2010
Accepted 10 February 2010
Available online 12 March 2010

Keywords:
Vegetation pattern
Cross-scale relationship
Anisotropic
Wavelet analysis
Sand dunes
Water gradient

ABSTRACT

Vegetation striped pattern is a common feature in semiarid and arid landscapes, which is seen as mosaics including vegetated and non-vegetated patches. Identifying scales of pattern in ecological systems and referring patterns to multi-scaled processes that create them are ongoing challenges. The aim of this paper is to study the vegetation patterns and their across-scale relationships between the vegetation and anisotropic topography (W–E and N–S) in 12 transects at Gurbantunggut desert. We used wavelet-based across-scale analysis for extracting information on scales of pattern for those transect data, evaluating their inherent structure, and inferring characteristics of the processes that imposed those patterns at across scales. The results show that, in W–E direction, the scales of vegetation pattern (*C. ewersmanniana* is at the scale 40 m, *H. ammodendron*, at 35 m) correspond to the dune ridge/dune valley sequences (appearing at distance of 40 m), and vegetation on mesoscale and large scale are significant cross-scale correlation with topography on mesoscale and large scale in all W–E transects. In N–S direction, there is an irregular pattern of vegetation along the N–S irregular topography, and no unified cross-scale relationships between topography and vegetation on different scales in different transects. Moreover, cross-scale correlation analysis between topography and vegetation provides further detail on hierarchical structure and specific scales in space that strongly influenced the larger patterns. Knowledge of the cross-scale relationships between topography and vegetation could lead to better understanding and management of biological resources in that region.

1. Introduction

Landscapes in arid and semiarid systems consist of a mosaic of vegetation patches, banded spatial patterns of vegetation are a central feature of these areas, called "tiger bush", dominated by different species, controlled by different processes (Peters et al., 2006). There is a continuing debate on the ecological processes responsible for vegetation spatial patterns (Li, 2000a,b; Liu et al., 2008). A number of processes impact on the vegetation patterns have been identified, such as water scarcity, plant competition over water resources, and redistribution of water by runoff and diffusion, and moreover associated with positive feedbacks between vegetation and its most limiting resource water (Liu et al., 2008; Peters and Havstad, 2006; Scheffer et al., 2005; von Hardenberg et al., 2001), climate (Adams and Carr, 2003; D'Odorico et al., 2005; Liu et al., 2008; Rodriguez-Iturbe et al., 1999), soil storage capacity, and rainfall interception (Isham et al., 2005; Liu et al., 2008; Rodriguez-Iturbe et al., 1999), vertical penetration and horizontal advection of water at the plant scale (Breshears and Barnes, 1999) and focused on the importance of water runoff at patch scales to landscape scale processes (Kefi et al., 2007; Ludwig et al., 2005; Peters and Havstad, 2006; Scanlon et al., 2007; Sole, 2007), and so on. Recent studies have showed that the competition for water and the positive feedback between water availability and plant growth are the underlying reasons for vegetation patterning (Liu et al., 2008; Peters and Havstad, 2006; Scheffer et al., 2005; von Hardenberg et al., 2001). Moreover, topography is important due to its influence on the water distribution, which could indirectly controls the vegetation patterns at different scales (Bloesch, 2008; Doble et al., 2006; Geertsema and Pojar, 2007; Inoue et al., 2008; Isselin-Nondedeu and Bedecarrats, 2007; Londono, 2008; Munoz-Reinoso and Novo, 2005; Stavi et al., 2008).

Research on key components of spatially heterogeneous landscapes has traditionally focused on detecting its patterns and processes, and obtaining detailed information of the importance of spatial pattern in landscapes at multiple scales (Breshears and Barnes, 1999; Munoz-Reinoso and Novo, 2005). However, a landscape pattern is spatially correlated and scale-dependent

* *Corresponding author*. Tel.: +86 13579751189.
E-mail address: liutong1968@yahoo.com.cn (T. Liu).

1476-945X/$ – see front matter © 2010 Elsevier B.V. All rights reserved.
doi:10.1016/j.ecocom.2010.02.009

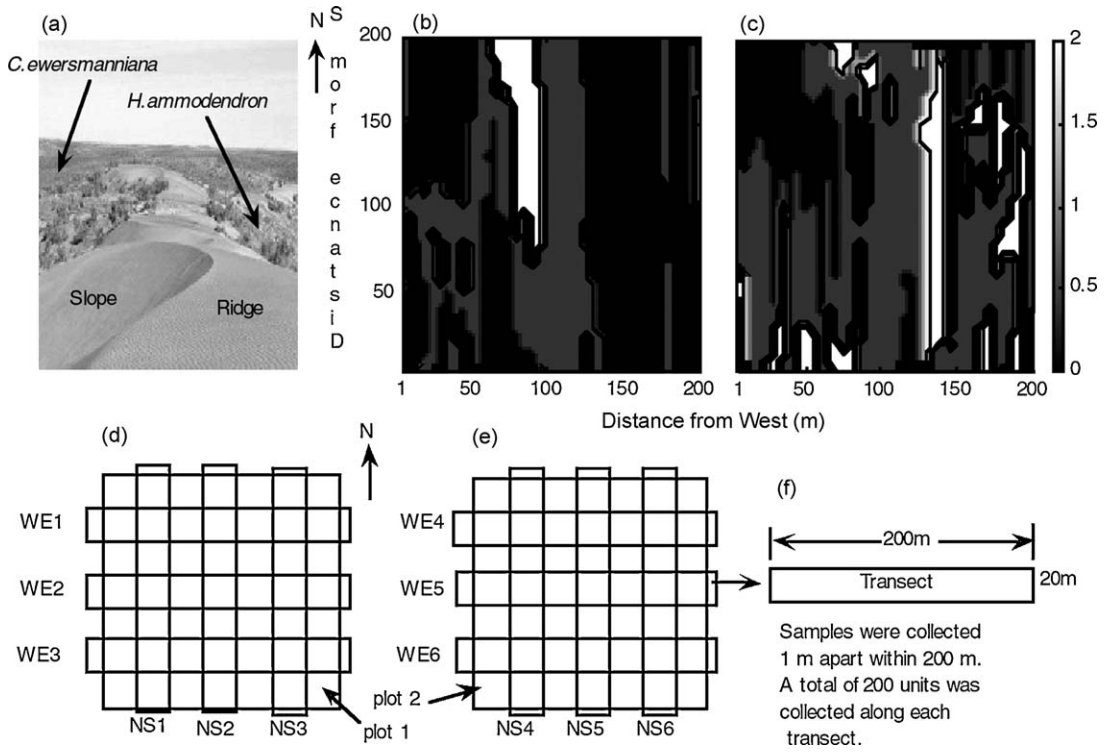

Fig. 1. Topographic map, and 12 transects of the two study plots. (a) Landscape of study area; (b) topography of plot 1; (c) topography of plot 2; (d) transects in plot 1; and (e) transects in plot 2.

(Breshears and Barnes, 1999; Wu, 2004), therefore, identifying ecological processes is dominant at different spatial scales that are the key property for understanding spatial ecological patterns (Munoz-Reinoso and Novo, 2005; Reitalu et al., 2008; Wu, 2004). Furthermore, interactions across spatial scales are common features of biological and ecological systems (Li, 2000a,b; Peters et al., 2004); previous studies rarely consider cross-scale relationships, and they assumed that the effects of ecological processes are uniformly important across scales. As a result, these deficiencies may limit the usefulness of studies (Breshears and Barnes, 1999; Francois et al., 2008; He et al., 2002; Jelinski and Wu, 1996; Kalwij et al., 2008; Millard, 2008; Munoz-Reinoso and Novo, 2005; Wu, 2004; Yao et al., 2006).

In this article, wavelet analysis was used to detect the scales of pattern for two dominant shrubs and topography at two mutually orthogonal directions (anisotropic topography is concerned) in Gurbantunggut desert, China. We examined the cross-scale associations between vegetation patterns and topography (which controls the vegetation pattern at different scales mediated through water gradient) in two mutually orthogonal directions (W–E and N–S) at a continuous spatial scale domain, and the difference at two directions.

1.1. Study area

Mosuowan is located in south boundary of Gurbantunggut desert, part of Junggar Basin in north Xinjiang, with an area of 48 000 km^2, which is mainly composed of stabilized longitudinal dunes (the length of dune is ranged from several hundred meters to some 10 km, nearly N–S trending; the height is 10–50 m; Fig. 1(a)) (Wang et al., 2003a,b). Remote from the oceans and surrounded by high mountains, the area has a typical continental climate marked primarily by low precipitation, low specific humidity, long winters and short springs and autumns, high solar radiation and a wide temperature range. The region receives an average annual precipitation of 200 mm and has a free surface evaporation of 1400–1700 mm. The annual average temperature is 6.6 °C. The frost-free period is about 150 days.

2. Methods

2.1. Sampling design and data collection

Two 4 ha square sample plots: plot 1 (86°09′29″E, 44°44′09″N; Fig. 1(b)) and plot 2 (86°05′40″E, 44°47′14″N; Fig. 1(c)) were established under clear-sky and dry in September 2005. In plot 1, three 200 m long, 20 m wide W–E transects were laid perpendicular to the stabilized dunes and three 200 m long, 20 m width N–S transects was laid parallel to the stabilized dunes (named as WE1–3, NS1–3, respectively, Fig. 1(d)). In addition, the same procedures were executed to plot 2 (named as WE4–6, NS4–6, respectively, Fig. 1(e)). Each transect was separated by 1 m and a total of 200 units was collected along the transect. In each unit, the density and habitats' topography (including ridge, slope, and valley) of the above-mentioned two shrubs were recorded.

2.2. Data preprocess

Data preprocessing was necessary before using wavelet analysis, it was done as follows:

The topography of the studied transects was divided into three topographic types (ridge, slope, and valley). To quantify the distribution of vegetation, the relative altitude was divided into three levels depended on topographic types (Xie et al., 2007). The vegetation density and topography along the transects were regarded as the fluctuation signals. All variables were assessed for normality, and transformed and standardized where the mean equals 0 and variance equals 1 as required to allow better identification of the relationships among the variables in

minimizing the overshadowing effects of certain variables having a wider range than others.

The data processes and drawing were accomplished by MATLAB6.5.

2.3. Data analysis

Wavelet analysis has been used to explore temporal scales of pattern in atmospheric flow (Gao and Li, 1993), spatial heterogeneity in the subsurface (Li, 1995), multiscale permeabilities in the subsurface (Li and Loehle, 1995), soil variability (Lark and Webster, 1999), understory plant diversity (Chen et al., 1999; Perry et al., 2002), properties of neutral landscapes (Keitt, 2000), plant productivity (Csillag and Kabos, 2002), multiscale patterns in microclimate along transects (Redding et al., 2003), solar activity (Rigozo et al., 2002; Rigozo et al., 2003), and concentrations of chlorophyll at the ocean surface (Nezlin and Li, 2003). Moreover, wavelet analysis has been used to evaluate the inherent structure in data and to infer characteristics of the processes that imposed those patterns (Saunders et al., 2005).

The integral wavelet transform is defined by:

$$(W_\psi f)(a,b) = \frac{1}{\sqrt{|a|}} \int f(t)\psi\left(\frac{t-b}{a}\right)dt \quad (1)$$

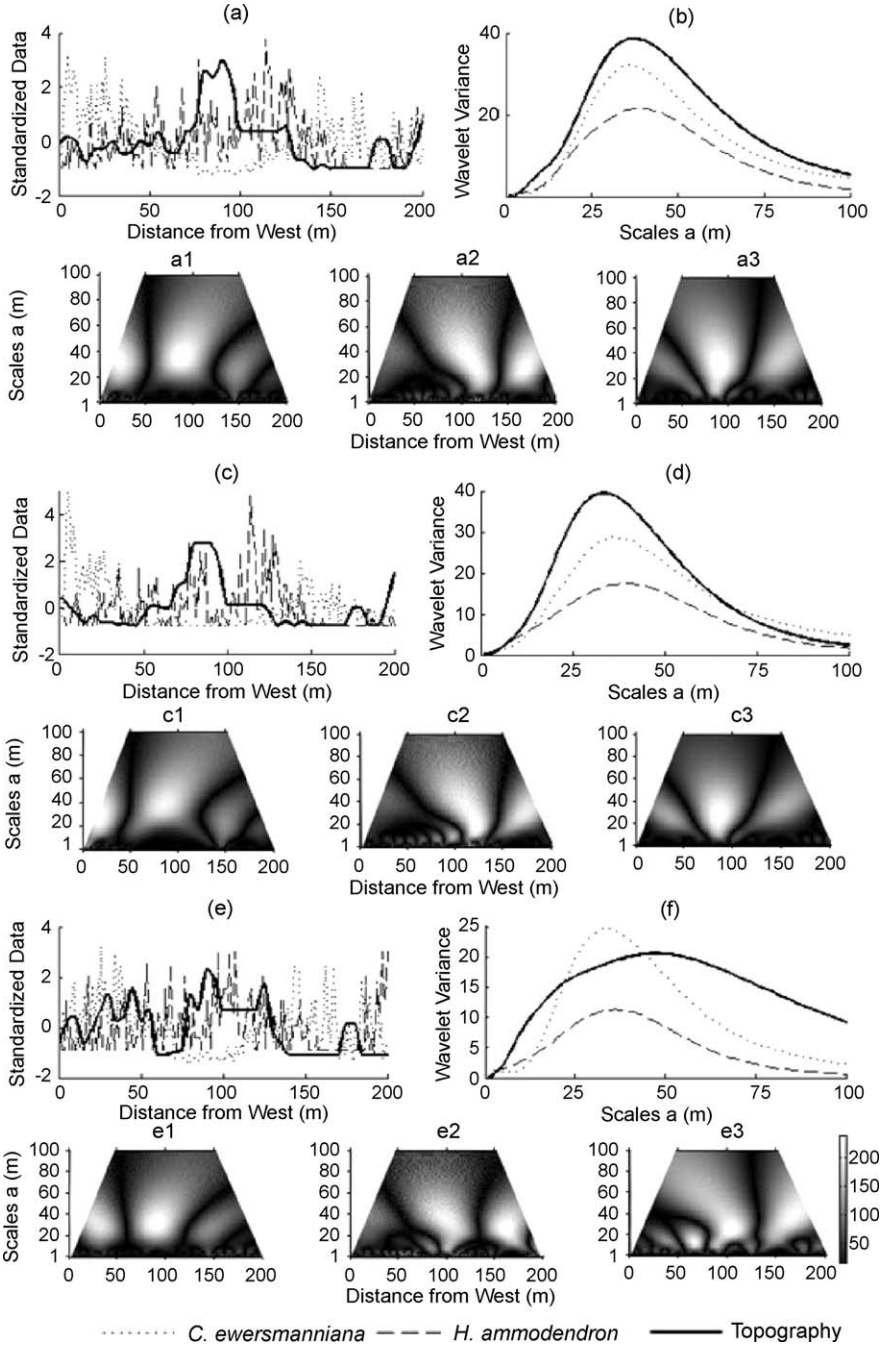

Fig. 2. Wavelet analysis for W–E transects in plot 1. ((a), (c), and (e)) Standardized data for topography and vegetation density for transect WE1–3, respectively; ((b), (d), and (f)) wavelet variance analysis for WE1–3, respectively; ((a1), (c1), and (e1)) the absolute values of wavelet coefficients of *C. ewersmanniana* for transect data in WE1–3, respectively; ((a2), (c2), and (e2)) the absolute values of wavelet coefficients of *H. ammodendron* for transect data in WE1–3, respectively; and ((a3), (c3), and (e3)) the absolute values of wavelet coefficients of topography for transect data in WE1–3, respectively.

where the shape (i.e., dimension of the analysis window) of the analyzing wavelet, $\psi(t)$, changes with scale, a, and the analyzing wavelet moves along the series of data, $f(t)$, centered at each point, b, along the data series (Gao and Li, 1993; Li and Loehle, 1995; Nezlin and Li, 2003). The appropriate wavelet can be chosen based on the type of data and the hypothesized pattern. Continuous wavelet transform was performed with a maximum scale of 100 m.

In our work, the "Mexican hat" wavelet $\psi(t') = (1 - t'^2)\exp(-t'^2/2)$ was used as the wavelet basis function, which is the second-order derivative of the Gaussian function defined within $-4 \le t' \le 4$ (Nezlin and Li, 2003).

The wavelet (scale) variance (Dale and Mah, 1998; Li, 1995; Li and Loehle, 1995; Nezlin and Li, 2003; Rosenberg, 2004):

$$WV_f(a) = \frac{1}{T_2(a) - T_1(a)} \int_{T_1(a)}^{T_2(a)} [(W_\psi f)(a,b)]^2 db$$

Here $T_1(a)$ and $T_2(a)$ are the lower and upper ends of $(W_\psi f)(a,b)$ are computed for a given scale a. The $WV_f(a)$ is simply the average of the squares of the $(W_\psi f)(a,b)$ at every point along transection for a given scale. The scale corresponding to a peak in wavelet variance is an estimate of the scale of dominant structure within the data (Gao and Li, 1993; Li and Loehle, 1995; Nezlin and Li, 2003).

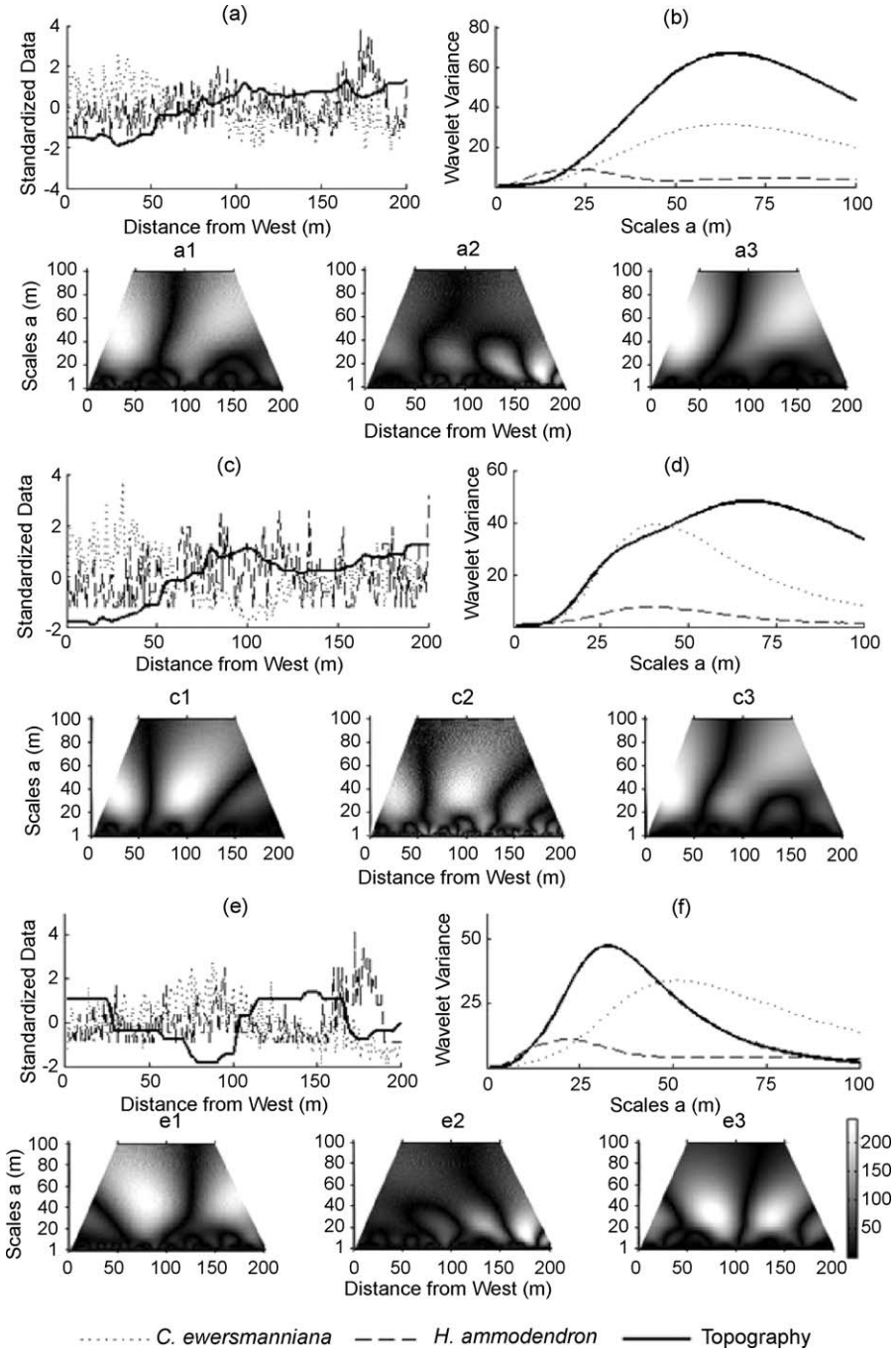

Fig. 3. Wavelet analysis for W–E transects in plot 2. ((a), (c), and (e)) Standardized data for topography and vegetation density for transect WE4–6, respectively; ((b), (d), and (f)) wavelet variance analysis for WE4–6, respectively; ((a1), (c1), and (e1)) the absolute values of wavelet coefficients of *C. ewersmanniana* for transect data in WE4–6, respectively; ((a2), (c2), and (e2)) the absolute values of wavelet coefficients of *H. ammodendron* for transect data in WE4–6, respectively; and ((a3), (c3), and (e3)) the absolute values of wavelet coefficients of topography for transect data in WE4–6, respectively.

Table 1
Dominant scales determined by wavelet variance for transect data.

Transect	Scale of pattern detected (m)		
	Topography	*C. ewersmanniana*	*H. ammodendron*
WE1	37	36	39
WE2	34	36	36
WE3	43	33	36
WE4	52	53	30
WE5	54	40	39
WE6	33	45	31
NS1	12, 66	25	28, 80
NS2	12	11, 61	30
NS3	13, 61	24, 61	73
NS4	21, 69	39	45
NS5	59	43	58
NS6	23	48	39

Position variance (Dale and Mah, 1998; Rosenberg, 2004):

$$WP_f(b) = \frac{1}{T_2(b) - T_1(b)} \int_{T_1(b)}^{T_2(b)} [W_\psi f(a,b)]^2 da$$

Here $T_1(b)$ and $T_2(b)$ are the lower and upper ends of $(W_\psi f)(a, b)$ across scales a at given point b. The $WP_f(b)$ is simply the average of the squares of the $(W_\psi f)(a, b)$ across scales at any one position b in time or space. It suggests features that produce high variance in the data (Dale and Mah, 1998; Rosenberg, 2004; Saunders et al., 2005). Peaks of position variance are also used to detect sudden changes (either increase or decrease) in the data series (Bradshaw and Spies, 1992; Redding et al., 2003; Saunders et al., 2005).

Wavelet analysis was performed in MATLAB 6.5.

3. Results

3.1. Scale of pattern detected in W–E transect

We calculated wavelet variance to examine the average contribution of the coefficients at each scale to data structure. We used position variance, whose strong peaks indicated the sudden changes (either increase or decrease) of data, to find locations within the series of data points that had relatively strong influences on the overall pattern averaged across scales (Saunders et al., 2005).

Fig. 2(a) illustrated the original pattern on vegetation and topography in transect WE1. Fig. 2(b) showed the profile of wavelet variance along the scale in transect WE1. The peaks of wavelet variance were often used as an estimate of the scale of pattern (Gao and Li, 1993; Li and Loehle, 1995). For topography in WE1, the peak of wavelet variance appeared at scale $a = 37$ m, which suggested that scale $a = 37$ m is the dominant scale for topography. In the same way, for *C. ewersmanniana* and *H. ammodendron* in WE1, wavelet variance indicated scales of pattern at 37 m and 39 m, respectively.

For WE2 (Fig. 2(c), (d), and (c1–3)), WE3 (Fig. 2(e), (f), and (e1–3)), WE4 (Fig. 3(a), (b), and (a1–3)), WE5 (Fig. 3(c), (d), and (c1–3)), WE6 (Fig. 3(e), (f), and (e1–3)), the results were almost the same as that in WE1: the scales of pattern for topography in WE2–6 were 34 m, 43 m, 52 m, 54 m, 33 m, respectively (Table 1); the scales of pattern for *C. ewersmanniana* in WE2–6 were 36 m, 33 m, 53 m, 40 m, 45 m, respectively (Table 1); the scales of pattern for *H. ammodendron* in WE2–6 were 36 m, 36 m, 30 m, 39 m, 31 m, respectively (Table 1; hereafter the scales range in 30–60 m was called as mesoscale; the scales smaller and larger than the mesoscale were called small scale and large scale, respectively).

The position variance of topography in WE1 showed a strong peak at 100 m, and lesser peaks were appeared at 66 m and 177 m. There are also some smaller position variances at 41 m and 155 m (Table 2). For *C. ewersmanniana* in WE1, position variance showed three relatively strong peaks at 19 m, 89 m and 146 m. For *H. ammodendron* in WE1, the position variance was highest at 93 m. Lesser peaks were apparent at 120 m, 167 m and 197 m.

All the peaks of position variance were listed in Table 2.

3.2. Scale of pattern detected in N–S transect

Scale of pattern in N–S transect was also analyzed by wavelet variance (Figs. 4 and 5, Table 1). Wavelet variance showed that there was only one dominant scale in NS2 (12 m), NS4 (59 m), and NS6 (23 m), but two dominant scales in NS1 (at 12 m and 66 m), NS3 (at 13 m and 61 m), NS4 (at 21 m and 69 m), which meant that dune ridge/dune valley sequence alternated irregularly in N–S transect, instead of having stable period like W–E transect. Along with topography variation, the heterogeneities in vegetation patterns increased in N–S transect and the scale was not stable. The vegetation pattern in NS1–3 had two dominant scales. For the same vegetation, its dominant scales varied greatly among transects in N–S, whereas these scales were almost the same in W–E transects. More peaks in the position variance of topography indicated that the heterogeneities in topography increased (Table 2). The results about vegetation also showed more peaks of position variance (Table 2).

3.3. Cross-scale correlation between vegetation and topography

To explore the relationships between vegetation and topography, cross-scale correlation analysis of wavelet coefficients at

Table 2
Locations of peaks of position variance for transect data.

Transect	Locations of peaks of position variance (m)		
	Topography	*C. ewersmanniana*	*H. ammodendron*
WE1	66^2, 100^1, 155^4, 177^3	19^3, 89^2, 146^1	93^1, 120^4, 167^2, 197^3
WE2	38^2, 86^1, 100^3, 148^4	16^3, 85^2, 149^1	100^1, 120^2, 172^3
WE3	39^4, 67^1, 105^3, 178^2	31^3, 91^2, 144^1,	87^4, 102^1, 165^2, 198^3
WE4	23^3, 56^4, 145^1, 174^2	25^3, 42^4, 141^2, 162^1	83^4, 146^1, 177^3, 195^2
WE5	28^3, 80^2, 143^1	24^3, 92^1, 128^2	95^1, 152^2
WE6	17^3, 72^2, 137^1, 182^4	42^2, 58^4, 83^3, 97^5, 166^1	93^4, 137^2, 176^3, 197^1
NS1	11, 36, 49, 67, 119^3, 134^2, 158^1	7, 49, 107^2, 155^1, 178^3	22, 62^2, 123^1, 167^3
NS2	10, 36^2, 134^1, 156^3, 179, 197	7^1, 20, 30, 51^2, 159^3	49^3, 70, 113^1, 120, 130, 159^2
NS3	23^3, 71, 116^2, 158^1, 184	59^2, 127^3, 151^1, 159, 177	21^3, 128^1, 168^2
NS4	18^3, 48^1, 153^2, 185	48, 103^2, 112^1, 175^3	80^2, 165^1, 198^3
NS5	39^1, 121^3, 185^2	52^1, 83^3, 92^2, 102, 166	47, 128^3, 162^2, 198^1
NS6	24^6, 56^5, 77^4, 109^3, 145^2, 187^1	47, 120^3, 138^2, 177^1	15, 83^1, 103^2, 122^3

$^{1-6}$the numeric superscript denotes the order of peaks. For example, 100^1 is the maximum peak and 155^4 is the fourth peak.

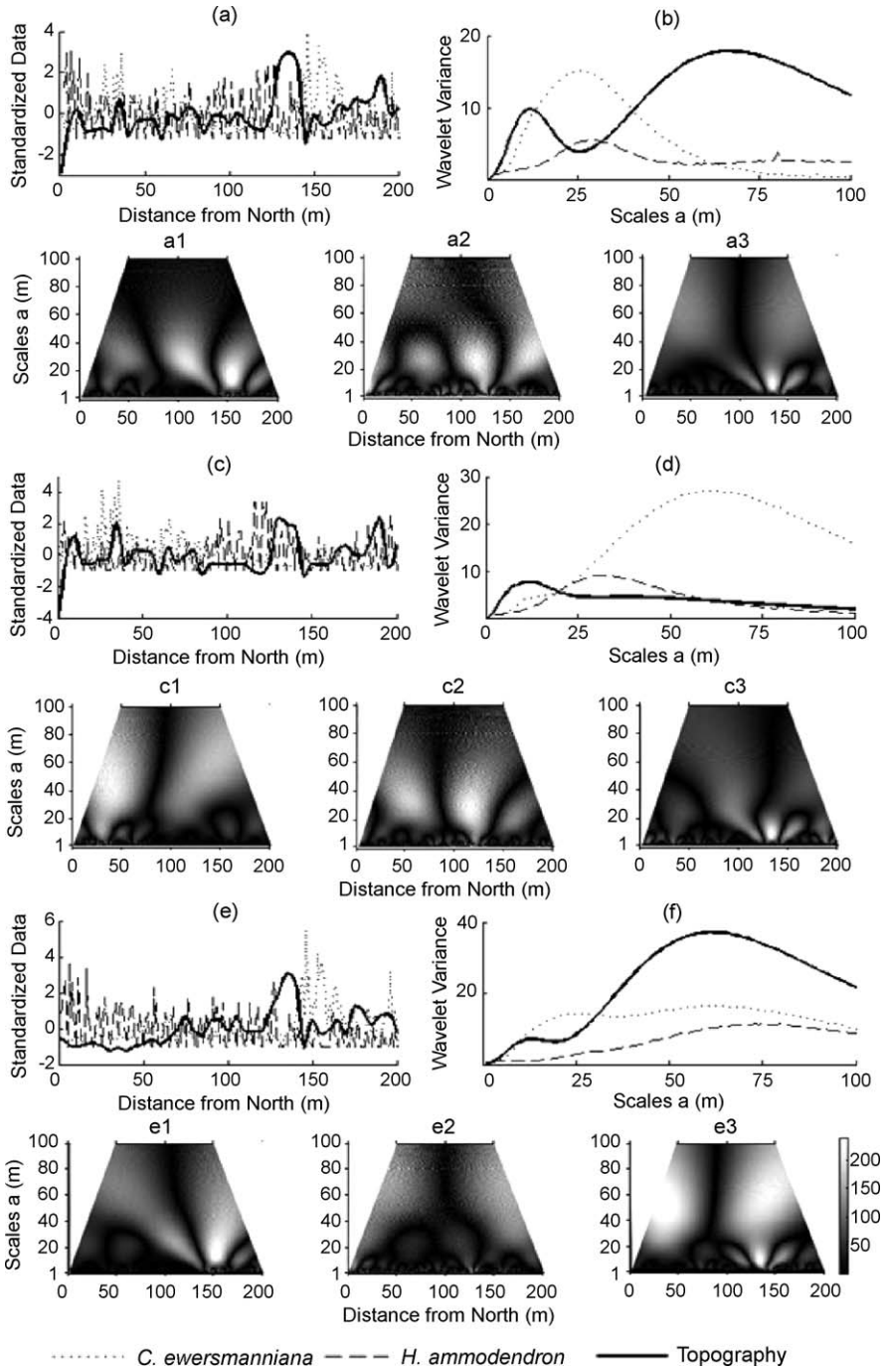

Fig. 4. Wavelet analysis for N–S transects in plot 1. ((a), (c), and (e)) Standardized data for topography and vegetation density for transect NS1–3, respectively; ((b), (d), and (f)) wavelet variance analysis for NS1–3, respectively; ((a1), (c1), and (e1)) the absolute values of wavelet coefficients of *C. ewersmanniana* for transect data in NS1–3, respectively; ((a2), (c2), and (e2)) the absolute values of wavelet coefficients of *H. ammodendron* for transect data in NS1–3, respectively; and ((a3), (c3), and (e3)) the absolute values of wavelet coefficients of topography for transect data in NS1–3, respectively.

different scales was performed (Fig. 6). The Spearman correlation coefficients were calculated and plotted with different colors.

In W–E direction, Fig. 6(a) illustrated the cross-scale correlation relationships between *C. ewersmanniana* and topography in six W–E transects. For WE1, topography and *C. ewersmanniana* were significantly negative cross-scale correlated at mesoscale (dark blue region in Fig. 6(a)-WE1). The results of WE2 and WE3 were nearly the same as WE1, as illustrated in Fig. 6(a). In WE4, topography and *C. ewersmanniana* were significant negative cross-scale correlated at mesoscale and large scale (dark blue region of Fig. 6(a)-WE4). The results of WE5 and WE6 were nearly the same as WE4 (dark blue region of Fig. 6(a)-WE5 and WE6).

Moreover, *H. ammodendron* and topography in W–E direction were significantly positive cross-scale correlated at mesoscale and large scale. But topography at small scale was not significant by correlated with *H. ammodendron* at all scales. Besides, *H. ammodendron* at small scale was not significantly correlated with topography at all scales (dark red region of Fig. 6(b)-WE1). The results were almost the same for the six W–E transects, as illustrated in Fig. 6(b) (dark red region of Fig. 6(b)-WE1–6).

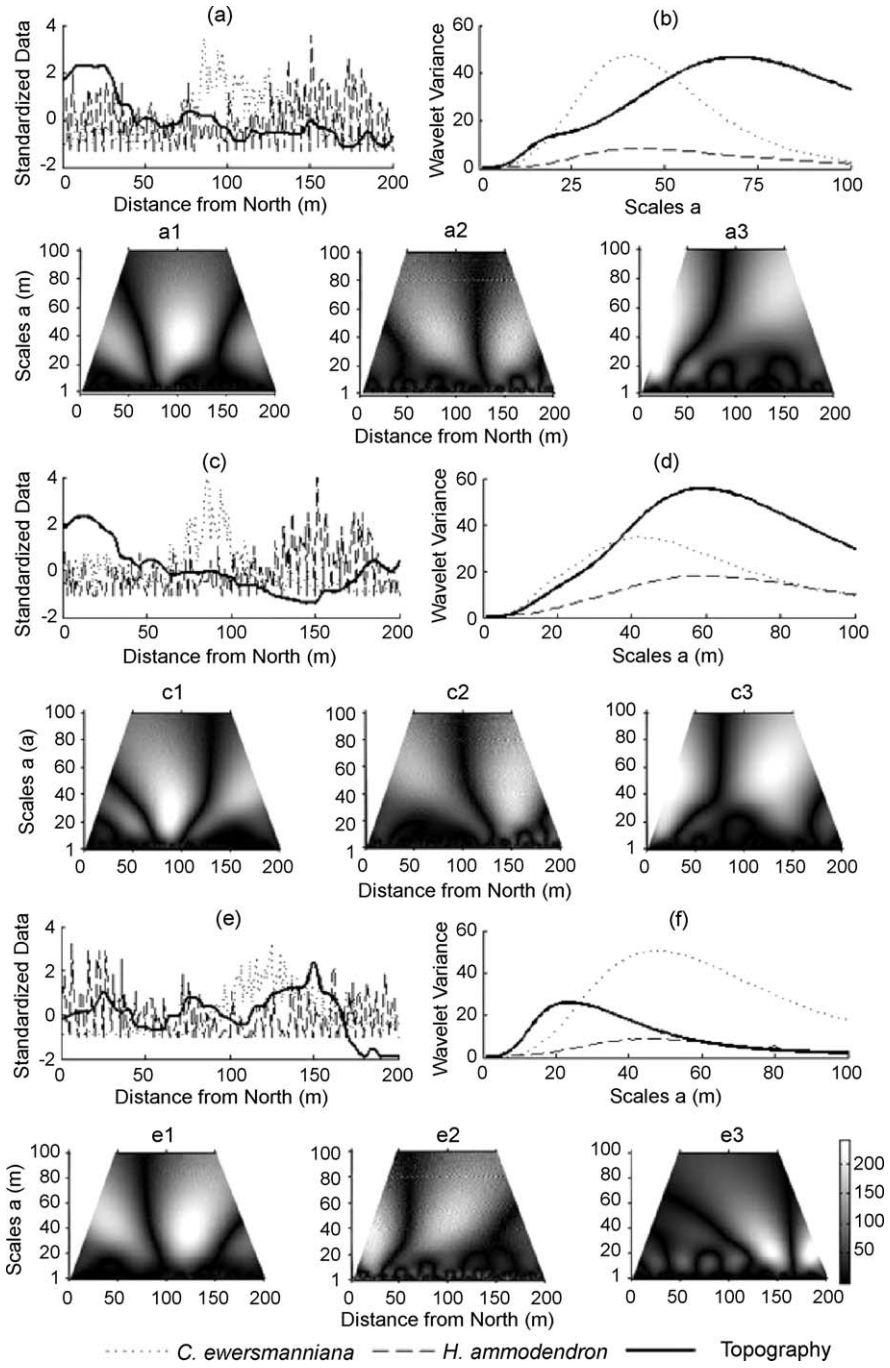

Fig. 5. Wavelet analysis for N–S transects in plot 2. ((a), (c), and (e)) Standardized data for topography and vegetation density for transect NS4–6, respectively; ((b), (d), and (f)) wavelet variance analysis for NS4–6, respectively; ((a1), (c1), and (e1)) the absolute values of wavelet coefficients of *C. ewersmanniana* for transect data in NS4–6, respectively; ((a2), (c2), and (e2)) the absolute values of wavelet coefficients of *H. ammodendron* for transect data in NS4–6, respectively; and ((a3), (c3), and (e3)) the absolute values of wavelet coefficients of topography for transect data in NS4–6, respectively.

Therefore, the patterns of *C. ewersmanniana* and *H. ammodendron* in W–E direction were controlled by topography across mesoscale and large scale.

In N–S direction, topography and *C. ewersmanniana* were significantly negative cross-scale correlated at small scale in NS1 (dark blue region of Fig. 6(c)-NS1), and negative cross-scale correlated at large scale (dark blue region of Fig. 6(c)-NS2) but positive cross-scale correlated at small scale in NS2 (red region of Fig. 6(c)-NS2). In NS3, there was significant negative cross-scale correlated at small scale but significant positive cross-scale correlated at large scale (dark red region of Fig. 6(c)-NS3). In NS4, there was significant positive cross-scale correlated at small scale (red region of Fig. 6(c)-NS4). Topography and *C. ewersmanniana* were significant positive cross-scale correlated at large scale in NS5 (dark red region of Fig. 6(c)-NS5), and were significant positive cross-scale correlated at small and mesoscale in NS6 (dark red region of Fig. 6(c)-NS6).

For topography and *H. ammodendron*, as illustrated in Fig. 6(d), at large scale in NS1, NS3–5 (dark blue region of Fig. 6(d)-NS1, NS3–5), there were significantly negative cross-scale correlated, and no significant negative cross-scale correlated at mesoscale in NS6 (Fig. 6(d)-NS6); but at large scale in NS2, there were

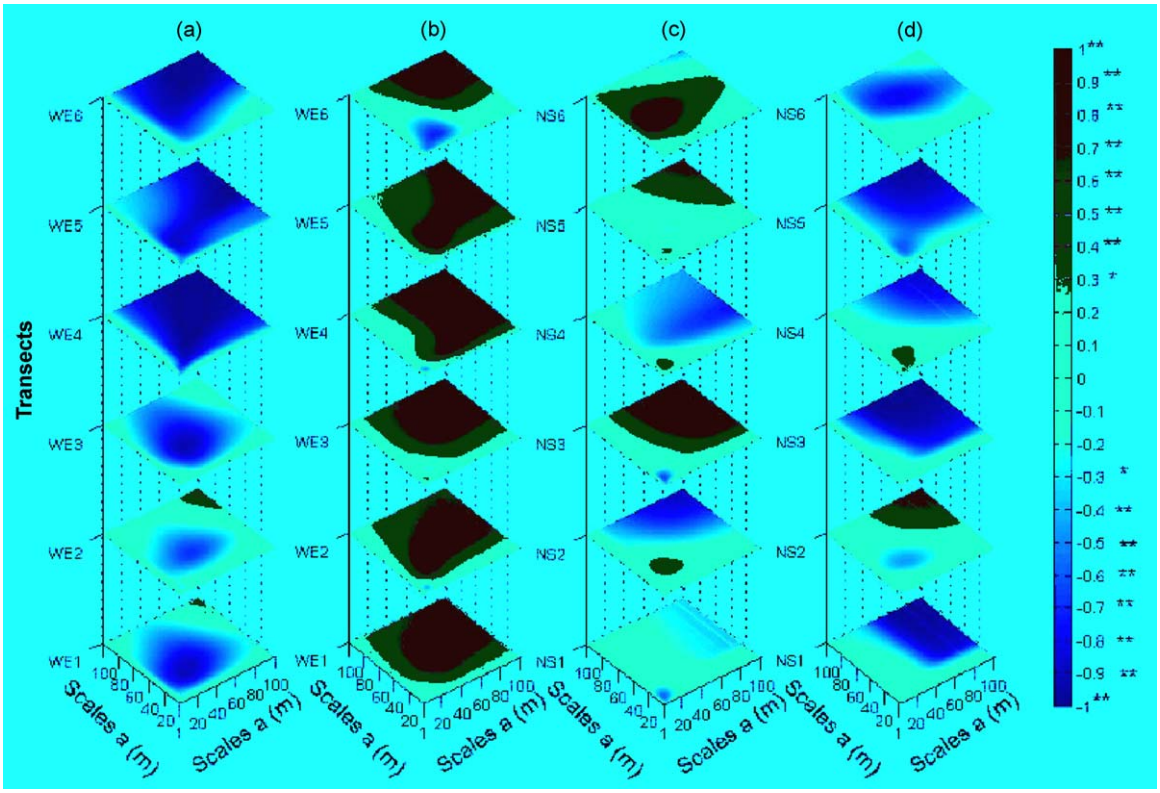

Fig. 6. Cross-scale correlation of wavelet coefficients between topography (*x*-axis) and vegetation (*y*-axis). (a) Topography and *C. ewersmanniana* in W–E direction; (b) topography and *H. ammodendron* in W–E direction; (c) topography and *C. ewersmanniana* in N–S direction; and (d) topography and *H. ammodendron* in N–S direction. *Significant correlation at the 0.05 level (two-tailed), and **significant correlation at the 0.01 level (two-tailed).

significant positive cross-scale correlated (dark red region of Fig. 6(d)-NS2).

Therefore, different transects had different results in N–S direction, but topography also controlled the pattern of *C. ewersmanniana* and *H. ammodendron*.

In summary, our study showed the regular vegetation along the W–E was controlled by regular topography across mesoscale and larger scales. But in N–S direction, the phenomenon was rather different because of the irregular topography.

4. Conclusion and discussion

Topographic constraint has a spatial structure. As a result, the processes, influenced by this constraint, instead of occurring in a spatially isotropic manner, become spatially oriented (Lefever and Lejeune, 1997). As anisotropic topography was concerned, the statistical analysis of topography and vegetation of two mutually orthogonal directions on cross-scale revealed the following conclusions.

1. In W–E direction, the scales of vegetation pattern (*C. ewersmanniana* at 40 m, *H. ammodendron* at 35 m, detected by wavelet variance analysis) corresponded to the dune ridge/dune valley sequence (appearing at distance of 40 m).In N–S direction, there were irregular patterns of vegetation along the N–S irregular topography.Previous studies showed that, within dune systems, geomorphology, through the alternation of dune ridges and valleys, produces a characteristic banded pattern due to differences in water gradients (Dickinson and Mark, 1994; Munoz Reinoso, 2001; Munoz-Reinoso and Novo, 2005). Therefore, both topography and vegetation had dominant scales in W–E transect, which might related with the alternation of dune ridges and valleys and the stable period of dune ridge and dune valley sequence. Due to the period of dune ridge/dune valley sequence in W–E direction, the vegetation patterns was controlled by topography mediated through water gradients, and further form the similar period.
2. For cross-scale relationships between topography and vegetation, there were many differences between W–E and N–S directions. In W–E direction, topography at mesoscale and large scale was significantly correlated with vegetation at mesoscale and large scale. But in N–S direction, there was no unified relationships between topography and vegetation on different scales in different transects. The cross-scale relationships between topography and vegetations provided detailed information about the relationships between underlying processes and spatial patterns.

Therefore, in W–E direction, vegetation pattern is controlled by the regular topography at mesoscale. However, the topography is irregular in N–S direction with increasing heterogeneity. The effect of topography on vegetation pattern is different: topography at small scale is negatively (e.g. *C. ewersmanniana* in NS1) or positively (e.g. *C. ewersmanniana* in NS2, NS4, and NS5) related with vegetation pattern at small scale, and negatively (e.g. *H. ammodendron* in NS1 and NS3–5) or positively (e.g. *C. ewersmanniana* in NS3) related with vegetation pattern at large scale.

Spatial vegetation patterns are an intriguing natural phenomenon, widespread in arid regions. This work has allowed the detection of multiple scales of pattern which are due to topographical factors. However, at regional scale, other spatial processes such as drought, and climate, operate which cannot be detected through our sampling design. These themes also need to be studied in the near future.

Acknowledgements

We acknowledge Bai-Lian Li from the University of California for his valuable suggestions on methods. The project was partially supported by National Key Project of Scientific and Technical Supporting Programs of Ministry of Science & Technology of China under grant no. 2007BAC17B03 and "Chunhui Projects" of Ministry of Education of China under grant no. Z2006-1-83014.

References

Adams, B., Carr, J., 2003. Spatial pattern formation in a model of vegetation–climate feedback. Nonlinearity 16, 53183–53188 PII S0951-7715(03).
Bloesch, U., 2008. Thicket clumps: a characteristic feature of the Kagera savanna landscape, East Africa. Journal of Vegetation Science 19, 31–44.
Bradshaw, G.A., Spies, T.A., 1992. Characterizing canopy gap structure in forests using wavelet analysis. Journal of Ecology 80, 205–215.
Breshears, D.D., Barnes, F.J., 1999. Interrelationships between plant functional types and soil moisture heterogeneity for semiarid landscapes within the grassland/forest continuum: a unified conceptual model. Landscape Ecology 14, 465–478.
Chen, J.Q., Saunders, S.C., Crow, T.R., Naiman, R.J., Brosofske, K.D., Mroz, G.D., Brookshire, B.L., Franklin, J.F., 1999. Microclimate in forest ecosystem and landscape ecology—variations in local climate can be used to monitor and compare the effects of different management regimes. Bioscience 49, 288–297.
Csillag, F., Kabos, S., 2002. Wavelets, boundaries, and the spatial analysis of landscape pattern. Ecoscience 9, 177–190.
Dale, M.R.T., Mah, M., 1998. The use of wavelets for spatial pattern analysis in ecology. Journal of Vegetation Science 9, 805–814.
Dickinson, K.J.M., Mark, A.F., 1994. Forest–wetland vegetation patterns associated with a holocene dune-slack sequence, haast ecological district, South Western New-Zealand. Journal of Biogeography 21, 259–281.
Doble, R., Simmons, C., Jolly, I., Walker, G., 2006. Spatial relationships between vegetation cover and irrigation-induced groundwater discharge on a semi-arid floodplain, Australia. Journal of Hydrology 329, 75–97.
D'Odorico, P., Laio, F., Ridolfi, L., 2005. Noise-induced stability in dryland plant ecosystems. Proceedings of the National Academy of Sciences of the United States of America 102, 10819–10822.
Francois, C., Alexandre, L., Julliard, R., 2008. Effects of landscape urbanization on magpie occupancy dynamics in France. Landscape Ecology 23, 527–538.
Gao, W., Li, B.L., 1993. Wavelet analysis of coherent structures at the atmosphere forest interface. Journal of Applied Meteorology 32, 1717–1725.
Geertsema, M., Pojar, J.J., 2007. Influence of landslides on biophysical diversity—a perspective from British Columbia. Geomorphology 89, 55–69.
He, F.L., LaFrankie, J.V., Song, B., 2002. Scale dependence of tree abundance and richness in a tropical rain forest, Malaysia. Landscape Ecology 17, 559–568.
Inoue, T., Enoki, T., Tashiro, N., Sakuta, K., Inoue, S., 2008. Effects of topography and planted trees on the distribution of naturally regenerated broad-leaved trees in a 140-year-old *Cryptomeria japonica* plantation in northern Kyushu, Japan. Journal of Forest Research 13, 365–371.
Isham, V., Cox, D.R., Rodriguez-Iturbe, I., Porporato, A., Manfreda, S., 2005. Representation of space–time variability of soil moisture. Proceedings of the Royal Society A: Mathematical Physical and Engineering Sciences 461, 4035–4055.
Isselin-Nondedeu, F., Bedecarrats, A., 2007. Soil microtopographies shaped by plants and cattle facilitate seed bank formation on alpine ski trails. Ecological Engineering 30, 278–285.
Jelinski, D.E., Wu, J.G., 1996. The modifiable areal unit problem and implications for landscape ecology. Landscape Ecology 11, 129–140.
Kalwij, J.M., Milton, S.J., McGeoch, M.A., 2008. Road verges as invasion corridors? A spatial hierarchical test in an arid ecosystem. Landscape Ecology 23, 439–451.
Kefi, S., Rietkerk, M., Alados, C.L., Pueyo, Y., Papanastasis, V.P., ElAich, A., de Ruiter, P.C., 2007. Spatial vegetation patterns and imminent desertification in Mediterranean arid ecosystems. Nature 449, 213–215.
Keitt, T.H., 2000. Spectral representation of neutral landscapes. Landscape Ecology 15, 479–493.
Lark, R.M., Webster, R., 1999. Analysis and elucidation of soil variation using wavelets. European Journal of Soil Science 50, 185–206.
Lefever, R., Lejeune, O., 1997. On the origin of tiger bush. Bulletin of Mathematical Biology 59, 263–294.
Li, B.L., 1995. Wavelet analysis for characterizing spatial heterogeneity in the subsurface. Wavelet Applications in Signal and Image Processing III 2569, 736–746.
Li, B.L., 2000a. Fractal geometry applications in description and analysis of patch patterns and patch dynamics. Ecological Modelling 33, 33–50.
Li, B.L., 2000b. Why is the holistic approach becoming so important in landscape ecology? Landscape and Urban Planning 50, 27–41.
Li, B.L., Loehle, C., 1995. Wavelet analysis of multiscale permeabilities in the subsurface. Geophysical Research Letters 22, 3123–3126 (correction, 23, 1059–1061, 1996).
Liu, Q.X., Jin, Z., Li, B.L., 2008. Numerical investigation of spatial pattern in a vegetation model with feedback function. Journal of Theoretical Biology 254, 350–360.
Londono, A.C., 2008. Pattern and rate of erosion inferred from Inca agricultural terraces in and southern Peru. Geomorphology 99, 13–25.
Ludwig, J.A., Wilcox, B.P., Breshears, D.D., Tongway, D.J., Imeson, A.C., 2005. Vegetation patches and runoff-erosion as interacting ecohydrological processes in semiarid landscapes. Ecology 86, 288–297.
Millard, A., 2008. Semi-natural vegetation and its relationship to designated urban green space at the landscape scale in Leeds, UK. Landscape Ecology 23, 1231–1241.
Munoz-Reinoso, J.C., Novo, F.G., 2005. Multiscale control of vegetation patterns: the case of Donana (SW Spain). Landscape Ecology 20, 51–61.
Munoz Reinoso, J.C., 2001. Sequential pattern in the stabilized dunes of Donana Biological Reserve (SW Spain). Journal of Coastal Research 17, 90–94.
Nezlin, N.P., Li, B.L., 2003. Time-series analysis of remote-sensed chlorophyll and environmental factors in the Santa Monica-San Pedro Basin off Southern California. Journal of Marine Systems 39, 185–202.
Perry, J.N., Liebhold, A.M., Rosenberg, M.S., Dungan, J., Miriti, M., Jakomulska, A., Citron-Pousty, S., 2002. Illustrations and guidelines for selecting statistical methods for quantifying spatial pattern in ecological data. Ecography 25, 578–600.
Peters, D.P.C., Bestelmeyer, B.T., Herrick, J.E., Fredrickson, E.L., Monger, H.C., Havstad, K.M., 2006. Disentangling complex landscapes: new insights into arid and semiarid system dynamics. Bioscience 56, 491–501.
Peters, D.P.C., Havstad, K.M., 2006. Nonlinear dynamics in arid and semi-arid systems: interactions among drivers and processes across scales. Journal of Arid Environments 65, 196–206.
Peters, D.P.C., Pielke, R.A., Bestelmeyer, B.T., Allen, C.D., Munson-McGee, S., Havstad, K.M., 2004. Cross-scale interactions, nonlinearities, and forecasting catastrophic events. Proceedings of the National Academy of Sciences of the United States of America 101, 15130–15135.
Redding, T.E., Hope, G.D., Fortin, M.J., Schmidt, M.G., Bailey, W.G., 2003. Spatial patterns of soil temperature and moisture across subalpine forest-clearcut edges in the southern interior of British Columbia. Canadian Journal of Soil Science 83, 121–130.
Reitalu, T., Prentice, H.C., Sykes, M.T., Lonn, M., Johansson, L.J., Hall, K., 2008. Plant species segregation on different spatial scales in semi-natural grasslands. Journal of Vegetation Science 19, 407–416.
Rigozo, N.R., Nordemann, D.J.R., Echer, E., Zanandrea, A., Gonzalez, W.D., 2002. Solar variability effects studied by tree-ring data wavelet analysis. Solar Variability and Solar Physics Missions 29 PII S0273-1177(02)00245-4.
Rigozo, N.R., Vieira, L.E.A., Echer, E., Nordemann, D.J.R., 2003. Wavelet analysis of solar-ENSO imprints in tree ring data from Southern Brazil in the last century. Climatic Change 60, 329–340.
Rodriguez-Iturbe, I., Porporato, A., Ridolfi, L., Isham, V., Cox, D.R., 1999. Probabilistic modelling of water balance at a point: the role of climate, soil and vegetation. Proceedings of the Royal Society a-Mathematical Physical and Engineering Sciences 455, 3789–3805.
Rosenberg, M.S., 2004. Wavelet analysis for detecting anisotropy in point patterns. Journal of Vegetation Science 15, 277–284.
Saunders, S.C., Chen, J.Q., Drummer, T.D., Gustafson, E.J., Brosofske, K.D., 2005. Identifying scales of pattern in ecological data: a comparison of lacunarity, spectral and wavelet analyses. Ecological Complexity 2, 87–105.
Scanlon, T.M., Caylor, K.K., Levin, S.A., Rodriguez-Iturbe, I., 2007. Positive feedbacks promote power-law clustering of Kalahari vegetation. Nature 449, 209–214.
Scheffer, M., Holmgren, M., Brovkin, V., Claussen, M., 2005. Synergy between small- and large-scale feedbacks of vegetation on the water cycle. Global Change Biology 11, 1003–1012.
Sole, R., 2007. Ecology—scaling laws in the drier. Nature 449, 151–153.
Stavi, I., Ungar, E.D., Lavee, H., Sarah, P., 2008. Surface microtopography and soil penetration resistance associated with shrub patches in a semiarid rangeland. Geomorphology 94, 69–78.
von Hardenberg, J., Meron, E., Shachak, M., Zarmi, Y., 2001. Diversity of vegetation patterns and desertification. Physical Review Letters 87, 198101.
Wang, X.Q., Lei, J.Q., Jiang, J., Qian, Y.B., 2003a. Pattern of blown sand motion on longitudinal dune surface and its threat to linear engineering projects in Gurbantonggut desert, Xinjiang, China. Arid Land Geography 2, 143–149.
Wang, X.Q., Li, B.W., Zhang, Y.M., 2003b. Stabilization of dune surface and formation of mobile belt at the top of longitudinal dunes in Gurbantonggut Desert, Xinjiang. Journal of Desert Research 2, 126–131.
Wu, J.G., 2004. Effects of changing scale on landscape pattern analysis: scaling relations. Landscape Ecology 19, 125–138.
Xie, J.B., Liu, T., Wei, P., Jia, Y.M., Luo, C., 2007. Ecological application of wavelet analysis in the scaling of spatial distribution patterns of *Ceratoides ewersmanniana*. Acta Ecologica Sinica 27, 2704–2714.
Yao, J., Peters, D.P.C., Havstad, K.M., Gibbens, R.P., Herrick, J.E., 2006. Multi-scale factors and long-term responses of Chihuahuan desert grasses to drought. Landscape Ecology 21, 1217–1231.